THE JOURNAL OF PHYSICAL CHEMISTRY C

ARTICLE

pubs.acs.org/JPCC

Synthesis, Electrochemistry, and Electrogenerated Chemiluminescence of Azide-BTA, a D−A−π−A−D Species with Benzothiadiazole and *N*,*N*-Diphenylaniline, and Its Nanoparticles

Jungdon Suk,[†] Jian-Zhang Cheng,[‡] Ken-Tsung Wong,*[,‡] and Allen J. Bard*[,†]

[†]Center for Electrochemistry and Department of Chemistry and Biochemistry, The University of Texas at Austin, Austin, Texas 78712, United States

[‡]Department of Chemistry, National Taiwan University, 10617 Taipei, Taiwan

Supporting Information

ABSTRACT: We report the synthesis, electrochemistry, spectroscopy, and electrogenerated chemiluminescence (ECL) of a donor (D)−acceptor (A) molecule of form D−A−π−A−D, 4,4′-(7,7′-(9,9-bis(6-azidohexyl)-9*H*-fluorene-2,7-diyl)bis(benzo[c][1,2,5]thiadiazole7,4-diyl))bis(*N*,*N*-diphenylaniline) (**Azide-BTA**), and its organic nanoparticles (NPs). **Azide-BTA** consists of two 2,1,3-benzothiadiazole (A) and triphenylamine (D) groups at the ends bridged by a fluorene (π) moiety. Cyclic voltammetry (CV) of **Azide-BTA** showed a single reversible reduction wave (E^{o}_{red} = −1.48 V vs SCE) and two reversible oxidation waves ($E^{o}_{1,ox}$ = 0.92 V, $E^{o}_{2,ox}$ = 1.34 V vs SCE). The first oxidation and reduction waves were assigned two reversible, closely spaced one-electron transfers. **Azide-BTA** exhibited a large solvatochromic effect in the emission ranging from yellow (580 nm) to red (633 nm). The ECL spectrum resulting from the annihilation reaction showed a bright and single peak with a maximum at 652 nm in mixed solvent of acetonitrile and benzene (MeCN/Bz). Using a reprecipitation method, we prepared well-dispersed and spherical organic NPs of **Azide-BTA** in an aqueous solution. The size of the NPs was controlled by the preparation conditions, i.e., concentration of **Azide-BTA** in THF, water temperature, stirring rate, and method of dropping into water. The smallest and most stable size of the NPs was 16 ± 6 nm as analyzed by TEM. Those organic NPs showed stable and moderate intensity in annihilation ECL emission in an aqueous solution. With a coreactant, such as peroxydisulfate, an ECL spectrum was obtained that showed a single broader peak relative to that produced by annihilation from dissolved **Azide-BTA** molecules.

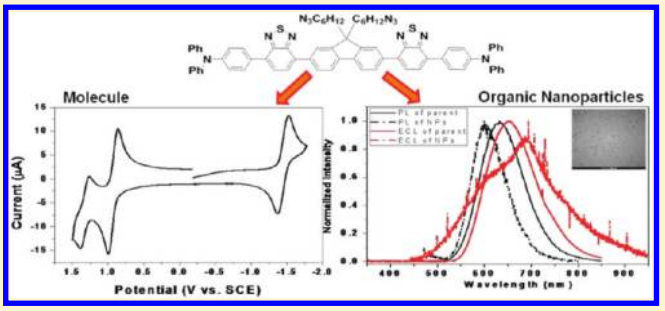

INTRODUCTION

We report the synthesis, electrochemical and photophysical characterization, and electrogenerated chemiluminescence (ECL) of a fluorescent molecule (**Azide-BTA**) and its NPs. **Azide-BTA** is a C2-symmetric donor−acceptor (DA) compound, consisting of two 2,1,3-benzothiadiazole groups as the acceptors and triphenylamine as the donors bridged by a fluorene moiety (Scheme 1). The compound is a D−A−π−A−D molecule, which shows reversibility upon electrochemical oxidation and reduction and intense red fluorescence.

We also fabricated stable organic nanoparticles (NPs) of **Azide-BTA** in an aqueous solution using a reprecipitation method and characterized their behavior in an aqueous solution. Metal and inorganic semiconductor NPs have been extensively investigated and show new physical phenomena, such as quantum confinement or finite size effects, distinct from the bulk materials.[1] In contrast to the extensive research that has been done on metal and inorganic semiconductor NPs, the study of organic NPs is still at an early stage. Organic NPs are of interest because of their diverse structures, the flexibility and ease in their synthesis, and a binding affinity that can be tailored toward various materials.[2] Organic NPs can be prepared in aqueous solution by solvent deposition in a vacuum chamber,[3] laser ablation,[4] sol−gel phase transitions,[5] and reprecipitation methods.[6] The main challenge is to control the NP size and shape and to understand how these affect the optical and other properties. A large size (hence small diffusion coefficient) and low concentration are obstacles in electrochemical measurements of organic NPs since the observed currents are small. ECL has the advantage of high sensitivity and low background, so that it is possible to see an ECL signal as a function of potential, even when an electrochemical signal cannot be detected, and use this to obtain information about potentials for oxidation and reduction. It is also very sensitive as an analytical method and has been used to investigate organic molecules[7] and several semiconductor NPs.[8] Few ECL studies of organic NPs, e.g., 9,10-diphenylanthracene (DPA) and rubrene[9] and spiro-BTA,[10] have been reported. We found **Azide-BTA** NPs to be well dispersed and spherical with relatively small diameters (<20 nm)

Received: June 15, 2011
Published: June 22, 2011

Scheme 1. Synthesis of Azide-BTA

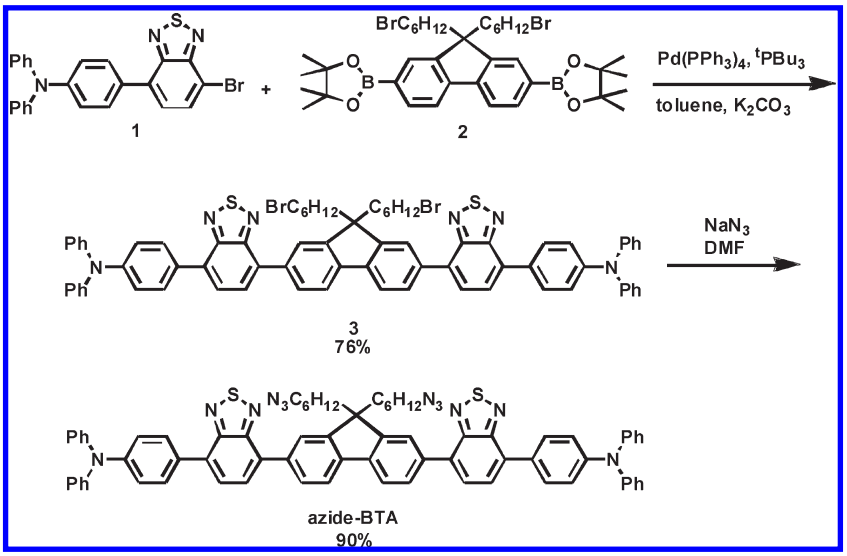

and a narrow size distribution in water. These produce sufficiently strong emission to measure the ECL spectrum with a coreactant in aqueous solutions. Using these as labels for biologically interesting molecules for aqueous analysis will be investigated.

EXPERIMENTAL SECTION

Materials. Unless otherwise noted, all reagents were used as received without further purification. Anhydrous acetonitrile (MeCN, 99.93%) and anhydrous benzene (Bz, 99.9%) were obtained from Aldrich (St. Louis, MO). Tetrahydrofuran (THF) and toluene were distilled under N_2 from sodium/benzophenone immediately prior to use. Tetra-*n*-butylammonium hexafluorophosphate ($TBAPF_6$) was obtained from Fluka and used as received. All solutions were prepared in a Ar atmosphere glovebox (Vacuum Atmospheres Corp., Hawthorne, CA) and placed in an airtight cell with Teflon cap for measurements completed outside the box.

The triphenylaminobenzothiadiazole (**1**)[11] and fluorene diboronic ester (**2**)[12] were synthesized according to published procedures. All commercially available compounds were used as received without further purification. Chromatography for purification was carried out with Merck silica gel for flash columns, and preparative thin-layer chromatography (TLC) was conducted on 1000 μm Whatman plates. ^{1}H and ^{13}C NMR spectra were recorded on a 400 MHz spectrometer at room temperature. High-resolution mass spectrometry (HRMS) was performed with Micromass ProSpec using fast atom bombardment (FAB).

Synthesis of Azide-BTA. To a solution of (**2**) (0.58 g, 0.98 mmol), (**1**) (0.7 g, 1.56 mmol), and tetrakis(triphenylphosphine) palladium (90 mg, 0.078 mmol) in toluene (50 mL) was added ^{t}PBu$_3$ (1.56 mL, 0.05 M in toluene) and K_2CO_3 (3 mL, 2 M) under N_2, and then the solution was stirred for one day at 85 °C. The mixture was partitioned between CH_2Cl_2 and brine. The organic solution was dried over $MgSO_4$ and concentrated under vacuum to get an orange solid. The orange solid was purified by chromatography over silica gel (mesh 40−63 nm elution with hexane/CH_2Cl_2 = 2/1) to get a light orange solid compound (**3**), 4,4′-(7,7′-(9,9-bis(6-bromohexyl)-9*H*-fluorene-2,7-diyl)bis(benzo[c][1,2,5]thiadiazole-7,4-diyl))bis(*N*,*N*-diphenylaniline) (0.74 g, 76%). Mp = 108−110 °C; IR (KBr) ν 3033, 2928, 2854, 2361, 1591, 1488, 1462, 1327, 1279, 1194, 1179 cm^{-1}; ^{1}H NMR ($CDCl_3$, 400 MHz) δ 8.05 (d, J = 7.6 Hz, 2H), 8.00 (s, 2H), 7.94−7.88 (m, 8H), 7.81 (d, J = 7.6 Hz, 2H), 7.33−7.22 (m, 20H), 7.10−7.06 (m, 4H), 3.29 (t, J = 6.8 Hz, 4H), 2.17 (m, 4H), 1.72−1.68 (m, 4H), 1.29−1.17 (m, 8H), 0.91−0.88 (m, 4H); ^{13}C NMR ($CDCl_3$, 100 MHz) δ 154.3, 154.2, 151.3, 148.1, 147.5, 140.8, 136.6, 133.0, 132.7, 130.9, 130.0, 129.4, 128.4, 128.1, 127.3, 124.9, 123.9, 123.3, 122.9, 120.1, 55.3, 40.1, 34.0, 32.6, 29.1, 27.7, 23.7; MS (m/z, FAB$^+$) 1244 (40), 1246 (100), 1248 (88); HRMS (m/z, FAB$^+$) calcd for $C_{73}H_{62}{}^{79}Br_2N_6S_2$ 1244.2844, found 1244.2810; calcd for $C_{73}H_{62}{}^{79}Br^{81}BrN_6S_2$ 1246.2824, found 1246.2808; calcd for $C_{73}H_{62}{}^{81}Br_2N_6S_2$ 1248.2803, found 1248.2843.

The mixture of (**3**) (0.54 g, 0.43 mmol) and NaN_3 (0.17 g, 2.6 mmol) was stirred in DMF (20 mL) at room temperature overnight. When the reaction was completed, the product was extracted with CH_2Cl_2, dried over $MgSO_4$, and concentrated under vacuum to get red crude. The crude was washed with hexane and MeOH to get a red solid (0.45 g, 90%), which is 4,4′-(7,7′-(9,9-bis(6-azidohexyl)-9*H*-fluorene-2,7-diyl)bis(benzo[c][1,2,5]thiadiazole-7,4-diyl))bis(*N*,*N*-diphenylaniline) (**Azide-BTA**). Mp = 102−104 °C; IR (KBr) ν 3033, 2926, 2853, 2090, 1589, 1510, 1486, 1461, 1326, 1274, 1194, 1178, 1073, 1026 cm^{-1}; ^{1}H NMR ($CDCl_3$, 400 MHz) δ 8.05 (d, J = 8.0 Hz, 2H), 8.00 (s, 2H), 7.94−7.87 (m, 8H), 7.81 (d, J = 7.2 Hz, 2H), 7.33−7.20 (m, 20H), 7.10−7.06 (m, 4H), 3.13 (t, J = 6.8 Hz, 4H), 2.17−2.13 (m, 4H), 1.46−1.41 (m, 4H), 1.27−1.17 (m, 8H), 0.91 (m, 4H); ^{13}C NMR ($CDCl_3$, 100 MHz) δ 154.6, 154.4, 151.5, 148.3, 147.7, 141.1, 136.8, 133.2, 132.9, 131.1, 130.2, 129.6, 128.6, 128.3, 127.5, 125.2, 124.1, 123.6, 123.1, 120.3, 55.5, 51.6, 40.4, 29.7, 28.9, 26.5, 24.0; MS (m/z, FAB$^+$) 1170 (60), 1290 (100); HRMS (FAB$^+$) m/z calcd for $C_{73}H_{62}N_{12}S_2$ 1170.4662, found 1170.4673.

Synthesis of Azide-BTA Nanoparticles. A reprecipitation method[6] was used for synthesis of **Azide-BTA** NPs by injecting 800 μL of **Azide-BTA** in THF (5×10^{-5} M) with a 50 μL microsyringe (Hamilton Co., Reno, NV) into 10 mL of warm (60−70 °C) deionized water under vigorous stirring. The resulting NP

dx.doi.org/10.1021/jp205621e |*J. Phys. Chem. C* 2011, 115, 14960–14968

solution was filtered through a 0.22 μm pore-size filter (Millex GP, PES membrane).

Characterization. The electrochemical cell consisted of a 2 mm diameter Pt disk (electrode area = 0.025 cm^2) inlaid in glass as a working electrode (WE), a Pt-coiled wire as a counter electrode (CE), a Ag wire as a quasi-reference electrode (QRE), and a Ag/AgCl reference electrode (for the nanoparticle experiment). The WE was bent at a 90° angle (J-type electrode) so that the electrode surface faced the detector. Before each experiment, the WE was polished on a felt pad with 1, 0.3, and 0.05 μm alumina (Buehler, Ltd., Lake Bluff, IL) suspensions in water, and then sonicated in DI water and ethanol for 1 min each. All electrodes were rinsed with acetone, dried in the oven, and transferred into the glovebox. Solutions for electrochemical measurements consisted of 0.5 mM **Azide-BTA** in a 1:1 (by volume) MeCN/Bz mixture as the solvent and 0.1 M $TBAPF_6$ as the supporting electrolyte. The preparation of all solutions was completed inside an inert Ar atmosphere glovebox, and the electrochemical cell was closed using a Teflon cap with a rubber O-ring to form an airtight seal for measurements outside the box. All potentials were calibrated against SCE by the addition of ferrocene serving as an internal standard at the end of all measurements, taking $E^{\circ}_{Fc/Fc+}$ = 0.342 V vs SCE.[13] Cyclic voltammograms (CVs) were obtained on a CH Instruments (Austin, TX) model 660 electrochemical workstation. Digital simulations of CVs were performed using DigiSim 3.03 (Bioanalytical Systems, Inc., West Lafayette, IN).

Spectroscopic experiments were done in a quartz cell. UV−vis spectra were recorded with a Milton Roy Spectronic 3000 array spectrophotometer. Fluorescence spectra were collected on a QuantaMaster spectrofluorimeter (Photon Technology International, Birmingham, NJ). For the ECL spectra, the detector was a charge-coupled device (CCD) camera (SPEC-32, Princeton Instruments, Trenton, NJ). The camera was cooled with liquid nitrogen between −100 and −120 °C, and the spectral wavelengths were calibrated with a mercury lamp. Faradaic current and ECL transients were simultaneously recorded by an Autolab electrochemical workstation (Eco Chemie, The Netherlands) coupled with a photomultiplier tube (PMT, Hamamatsu R4220p, Japan) held at −750 V with a high-voltage power supply (Kepco, Flushing, NY). ECL transients were generated by pulsing the electrode 80 mV beyond the diffusion-limited peak potentials for the first oxidation and the first reduction, respectively. Transmission electron microscopy (TEM) was performed with a Tecnai Spirit BioTwin microscope (FEI Company, The Netherlands) at an accelerating voltage of 80 kV. TEM samples were prepared by dropping 5 μL of fresh NP solution onto a 400 mesh carbon-coated copper TEM grid.

RESULTS AND DISCUSSION

Synthesis. The synthesis of **Azide-BTA** is depicted in Scheme 1. The Suzuki coupling reaction of the triphenylaminobenzothiadiazole intermediate (**1**) and fluorene diboronic ester (**2**) gave product (**3**) with a yield of 76% in the presence of a catalytic amount of tetrakis(triphenylphosphine) palladium and $^tPBu_3$ in toluene. After that, the mixture of (**3**) and NaN_3 under stirring in DMF produced the title compound **Azide-BTA** with an isolated yield of 90%.

Electrochemistry. Cyclic voltammetry was used to obtain information about the electrochemistry of the compounds, to determine the stability of the radical ions in solution, and to find

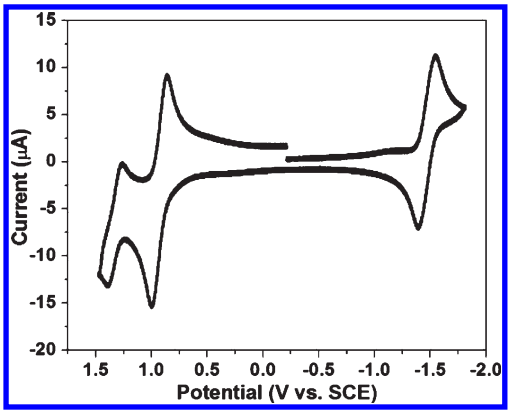

Figure 1. Cyclic voltammogram of 0.5 mM **Azide-BTA** in 1:1 Bz: MeCN with 0.1 M $TBAPF_6$. WE: Pt disk. CE: Pt coil. RE: Ag wire as a QRE. Scan rate was 0.5 V/s (surface area: 0.025 cm^2).

the energy of annihilation in ECL. In general, the peak current ratio (i_{pa}/i_{pc}) of all oxidation and reduction waves was approximately unity, indicating the absence of the following chemical reactions and good stability of the oxidized and reduced species. Moreover, scan rate studies showed that the peak currents of both oxidation and reduction waves of **Azide-BTA** were proportional to the square root of the scan rate ($\nu^{1/2}$) (see Figures S3 and S4 in the Supporting Information).

Figure 1 shows the CV of 0.5 mM **Azide-BTA** with 0.1 M $TBAPF_6$ as the supporting electrolyte in 1:1 anhydrous MeCN: Bz solution. The oxidation scan shows two oxidation waves at 0.92 V (E°_{ox1} vs SCE) and at 1.34 V (E°_{ox2} vs SCE) at a scan rate, ν, of 0.5 V/s. The peak current ($i_{pa} \sim 8$ μA) of the first wave is twice that of the second ($i_{pa} \sim 4$ μA), suggesting that the first oxidation process consists of two sequential, closely spaced, one-electron transfers assigned to the two terminal and noninteracting triphenylamine groups.

Figure 2 shows a comparison of experimental and simulated first oxidation CV of **Azide-BTA** at different scan rates from 50 mV/s to 2 V/s. Digital simulation of CVs with different scan rates helped to confirm the sequential one-electron transfer systems. Simulation was corrected for uncompensated resistance, R_u (1200 Ω), and double-layer capacitance, C_d (600 μF). The fit between experimental and simulated data for sequential electron transfer mechanisms was good. The results indicated that the diffusion coefficient from the simulation was 9×10^{-6} cm^2/s, E°_{ox1} = 0.92 V, and E°_{ox2} = 0.95 V vs SCE. In the simulation, all the electron-transfer reactions were considered fast so that the waves were diffusion controlled (simulation $k^{\circ} > 10^4$ s^{-1}, α = 0.5). The two triphenylamine groups are oxidized at similar potentials, suggesting negligible electronic interaction between these groups due to the intervening two 2,1,3-benzothiadiazole groups and the fluorene linker. The reversible second oxidation wave was a single electron transfer that can be attributed to the oxidation of the central fluorene moiety.[14]

The negative scan of **Azide-BTA** showed a reversible reduction wave at $E_{1/2}$ = −1.48 V vs SCE, which exhibited the same peak current (~8 μA) as the first oxidation wave. This is attributed to reduction of the two 2,1,3-benzothiadiazole groups, with two electron-withdrawing imine groups (C═N)[15] and a good acceptor compound, in a single reversible reduction peak, again suggesting little interaction across the fluorene linker. The reduction of **Azide-BTA** can be fit as two closely spaced

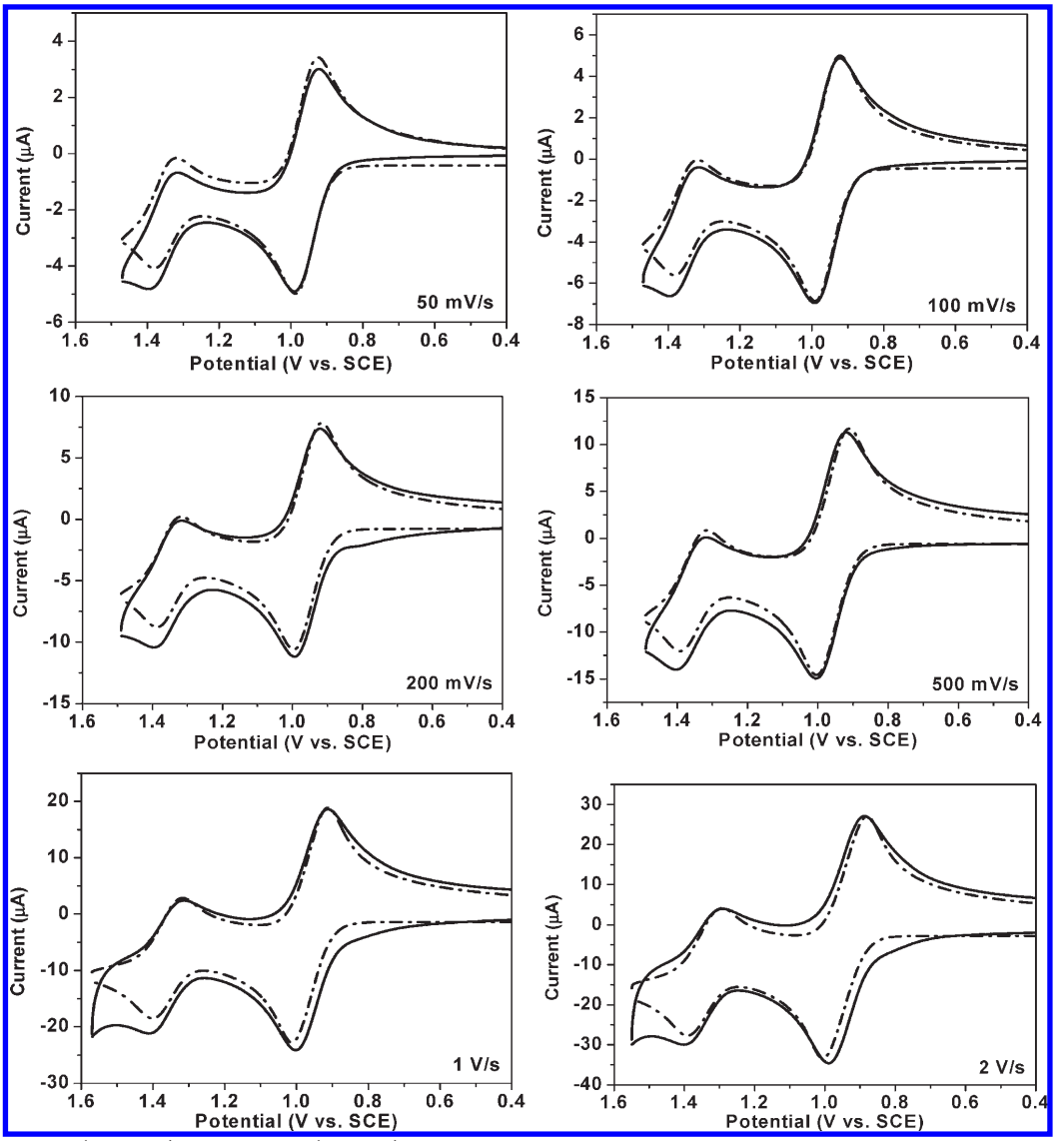

Figure 2. Experimental (solid line) and simulated (·—·—·) cyclic voltammograms of 0.5 mM **Azide-BTA** oxidation with scan rate from 50 mV/s to 2 V/s. The simulation mechanism involves two sequential one-electron oxidations in the first wave and a single one-electron oxidation in the second wave and is corrected for uncompensated resistance, R_u (1200 Ω), and double-layer capacitance, C_d (600 μF): $E^\circ_{1,ox}$ = 0.92 V, $E^\circ_{2,ox}$ = 0.95 V, $E^\circ_{3,ox}$ = 1.34 V vs SCE, $k^\circ \geq 10^4$ cm/s, α = 0.5.

nernstian waves at all scan rates, with potentials of $E^\circ_{1,red}$ = −1.44 V and $E^\circ_{2,red}$ = −1.49 V vs SCE and simulated assuming a fast heterogeneous electron transfer rate constant (simulation $k^\circ > 10^4$ s^{-1}) (Figure S5 in the Supporting Information).

Absorption and Emission Spectroscopy. Figure 3 shows the normalized UV−vis absorption (black line) and emission (blue line) spectra for **Azide-BTA** dissolved in 1:1 MeCN:Bz solution. The photophysical properties, absorption and emission maxima, fluorescence quantum yield, and the optical energy gap are summarized in Table 2. The absorbance of **Azide-BTA** exhibited two peaks at around 312 and 452 nm. The absorption peak at ∼312 nm is assigned to the $\pi-\pi^*$ local electron transition of the fluorene moiety,[16] and the longer wavelength corresponds to $\pi-\pi^*$ electron transition of the entire **Azide-BTA** backbone. The fluorescence of **Azide-BTA**, taken with excitation at the absorption maxima around 452 nm, featured an intense red emission peak with λ_{max} at 632 nm. The PL spectrum shows a large Stokes shift suggesting that the excitation caused an

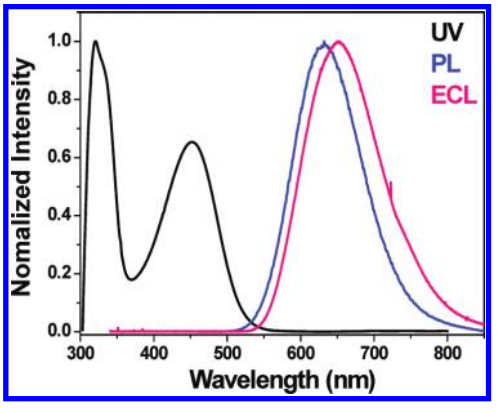

Figure 3. Absorbance (black), fluorescence (blue), and ECL (pink) spectra of 0.5 mM **Azide-BTA** in 1:1 Bz:MeCN by annihilation by stepping between the E_p^{red} −80 mV and the E_p^{ox} +80 mV. Integration time: 5 min. Slit width: 0.75 mm.

dx.doi.org/10.1021/jp205621e |J. Phys. Chem. C 2011, 115, 14960–14968

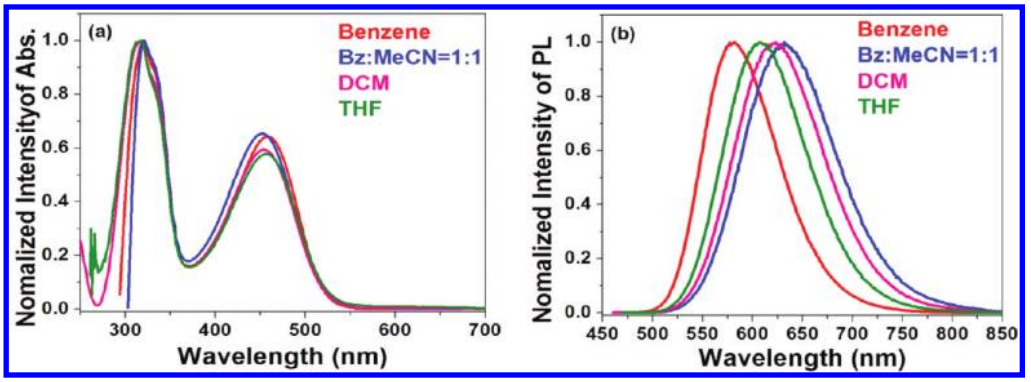

Figure 4. (a) Absorbance and (b) fluorescence spectra of **Azide-BTA** in various solvents. Emission spectra were excited at the absorption maxima (450 nm).

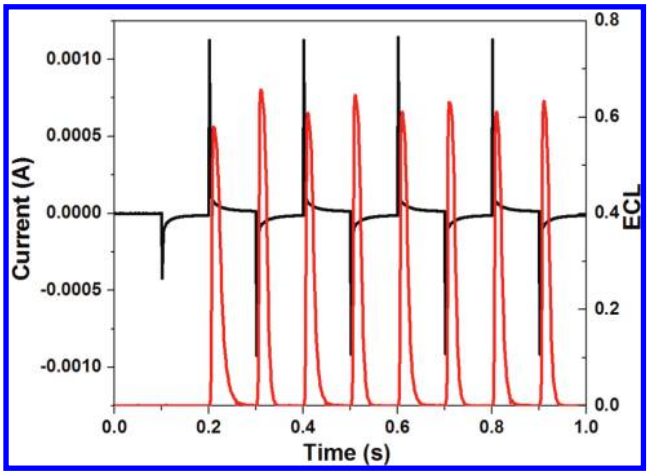

Figure 5. Transient ECL experiment, electrochemical current (black line), and ECL intensity (red line) for 0.5 mM **Azide-BTA**. Sampling time: 1 ms. Pulsing pattern: 0 V to negative ($E_{p,red}$ −80 mV) to anodic ($E_{p,ox}$ +80 mV). Pulse width is 0.1 s.

intramolecular electron transfer, and the emission involved a charge transfer process. This mechanism is supported by the strong dependence of the spectral properties on the solvent polarity,[17] resulting in a strong solvatochromic effect as shown in Figure 4(b) from yellow emission (580 nm) in benzene to red (633 nm) in 1:1 Bz:MeCN. The absorption spectra displayed little dependence of peak position on solvent, as shown in Figure 4(a) as expected from excitation mainly in the fluorene.[18]

Electrogenerated Chemiluminescence (ECL). Figure 3 shows the ECL spectrum (pink line) of **Azide-BTA** during repeated pulsing (pulse width = 0.1 s) between potentials where the oxidized and reduced forms were alternately produced (with a 5 min integration time). The potentials were repeatedly stepped from the reduction wave ($E_{1,pc}$ −80 mV) to the oxidation wave ($E_{1,pa}$ +80 mV), where both half reactions were diffusion limited. The ECL spectrum of **Azide-BTA** from the annihilation reaction produced strong red ECL that was easily visible with the naked eye. The ECL maximum was centered at 652 nm, which was red-shifted by 20 nm relative to the PL spectrum (blue line). The red-shift in the ECL spectrum can be explained by an inner-filter effect because of the difference of solution concentration used in PL and ECL and by the difference in resolution between the two instruments where the spectra

Table 1. Electrochemical Data

	$E_{1/2}$ (V vs SCE)		D	E_g[a]	E_{HOMO}[b]	E_{LUMO}[c]
chemical	reduction	oxidation	(cm^2/s)	(eV)	(eV)	(eV)
Azide-BTA	−1.48	0.92, 1.34	9×10^{-6}	−2.40	−6.08	−3.68

[a] From the CV. [b] The HOMO values are calculated based on the value of −4.8 eV in vacuum for ferrocene. [c] From the reduction wave.

were collected.[19] To estimate the stability of the radical ion species, potential pulsing ECL transients were collected. Figure 5 shows the symmetric current pulses and approximately equal ECL emission transient upon each anodic to cathodic pulse cycle with a 0.1 s pulse width. The ECL of **Azide-BTA** was stable for about 3000 s and then gradually decayed to low levels at about 5000 s. When the electrode was repolished and replaced into the solution, ECL emission was restored under the same pulsing conditions, suggesting the decay in emission was caused by the slow formation of a film on the electrode. The relative ECL quantum yield, $\Phi_{ECL,rel}$ was determined by comparing the number of photons emitted per electron or annihilation event with the standard ECL emitter, 9,10-diphenylanthracene (DPA). We found the ECL intensity to be about the same as DPA under the same conditions. Since the quantum yield of DPA in MeCN is ~8%,[20] the efficiency for **Azide-BTA** is roughly the same.

The enthalpy in the radical cation and anion annihilation can be calculated from the reversible potentials of redox couples with the equation, $-\Delta H_{ann} = -\Delta G - T\Delta S = (E^{o}_{A+/A} - E^{o}_{A/A-}) - 0.1$ eV.[7,21] ΔG is obtained from the difference between the standard potentials of the oxidation and reduction waves in the CV. Whether the enthalpy of annihilation is larger or smaller than the energy required to produce the excited singlet state from the ground state, E_s, the singlet excited state can be directly populated by radical ion annihilation, or the annihilation may still produce a triplet state.[22] If the radical ion annihilation energy is enough to populate an excited singlet state, this mechanism is called the S-route or "energy-sufficient system". The enthalpy of annihilation, $-\Delta H_{ann}$, for **Azide-BTA** calculated from the electrochemical data (shown in Table 1) is larger than the energy for an excited singlet state from the emission spectrum (Figure 3), so ECL via the S-route is a good possibility.

Formation of Organic NPs. The size of NPs was controlled by the preparation conditions, e.g., concentration of **Azide-BTA** in THF, water temperature, stirring rate, and method of introducing the THF solution into the water. The production of small

Table 2. Spectroscopic and ECL Data

chemical	$\lambda_{max(abs)}$ (nm)	$\lambda_{max(PL)}$ (nm)	Φ_{PL}[a]	$\lambda_{max(ECL)}$ (nm)	$\Phi_{r,ECL}$[b]	$-\Delta G_{ann}$[c] (eV)	$-\Delta H_{ann}$[d] (eV)	E_s[e] (eV)
Azide-BTA	312, 452	632	0.82	652	0.072	2.40	2.30	1.96
NPs	338, 483	586	0.14	670	-	-	-	-

[a] F_{PL} is the relative PL compared to DPA. $F_{PL,DPA} = 0.91$ in benzene. [b] $F_{r,ECL}$ is the relative ECL compared to DPA. $F_{ECL,DPA} = 0.014$. [c] $-\Delta G_{ann} = E_{pa}^{ox} - E_{pc}^{red}$. [d] $-\Delta H_{ann} = -\Delta G_{ann} - 0.1$. [e] $E_s = 1239.85/\lambda_{max(PL)}$ (nm).

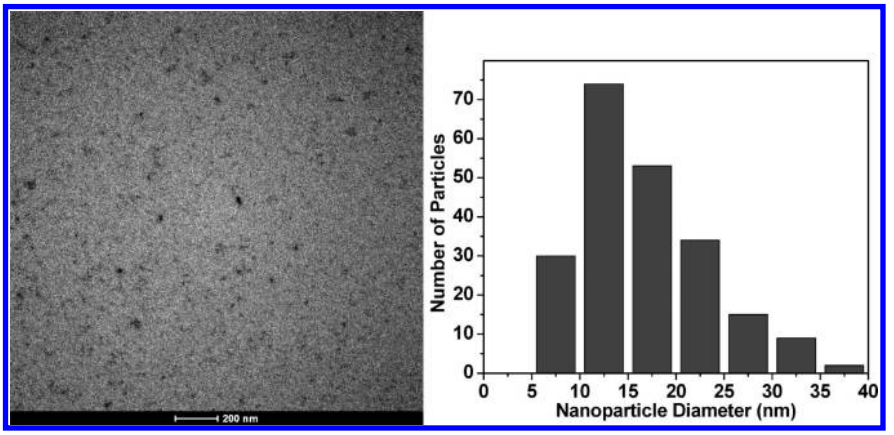

Figure 6. (Left) TEM image of organic NPs of **Azide-BTA** dispersed in water. (Right) Histogram of size distribution.

NPs with a narrow size distribution is important in increasing diffusion coefficients of the NPs. The size of the NPs mainly depends on the concentration of the parent molecule in THF and volume of the drops of the organic solutions added to the water. Figures S6 and S7 (Supporting Information) show the size distribution of NPs prepared under different conditions, e.g., a high concentration of the parent THF solution and room temperature water. When the parent concentration was lower and the drop volume was smaller, smaller NPs were produced. A higher water temperature (60 °C), which is just below the boiling point of THF, produces smaller NPs relative to those prepared at room temperature. Thus, when 0.5 μM **Azide-BTA** in THF solution was injected using a 50 μL syringe into 60 °C water with fast stirring, the average size of **Azide-BTA** NPs was around 16 nm. Figure 6 shows the TEM image of well-dispersed and spherical NPs with an average diameter of 16 nm. The size distribution indicates that the measured diameters ranged from a few to 40 nm. The size of the NPs was stable for one week under ambient conditions without addition of surfactant.

Microscopic and Spectroscopic Measurements. The optical properties of **Azide-BTA** NPs were obtained by absorption and emission spectroscopy. The absorption and emission spectra of **Azide-BTA** NPs compared to **Azide-BTA** in solution are shown in Figure 7. The absorbance maximum of **Azide-BTA** molecules in the THF/water mixture solution were located in 312 and 452 nm, while the absorbance maximum of NPs in water showed a red shift with peaks at 338 and 483 nm. The absorption spectrum of NPs showed a significant light scattering tail in the long wavelength region, as frequently seen with NPs.[23] Upon photoexcitation, the **Azide-BTA** NPs showed a single emission peak at 586 nm, blue-shifted by 10 nm as compared to **Azide-BTA** in a 1:9 THF:water solution. Unlike metal and inorganic semiconductor NPs, which show typical nanometer size dependence,

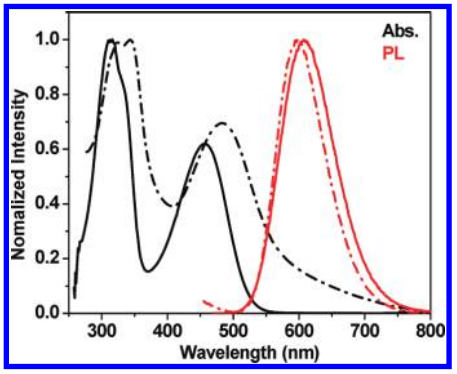

Figure 7. Spectra of absorbance (black) and fluorescence (red) of **Azide-BTA** in the mixed solution with 1:9 THF:water (solid line) and **Azide-BTA** NPs in water (dotted line). Emission spectra were excited at the absorption maximum (450 nm).

the spectroscopy of organic NPs has been the subject of relatively few studies. Only some organic NPs such as perylene,[24,25] phthalocyanine,[26,27] and pyrazoline NPs[28] have shown the size effects in the absorption and fluorescence spectra as well as fluorescence emission enhancement due to conformational changes of the molecules.[29] In the pyrazoline system, strong enhancement of the fluorescence intensity and efficiency as well as a wavelength shift to higher energy were observed with decreasing particle size. Unlike this recent case, the NPs of **Azide-BTA** showed little difference in the absorption and emission spectra of NPs compared to the molecules dissolved in an organic solvent and showed little effect of size with no enhancement of fluorescence intensity or efficiency (Figure S8 in the Supporting Information).

ECL of Organic NPs. Because of the limited potential window in aqueous solution and the low concentration of NPs, distinctive

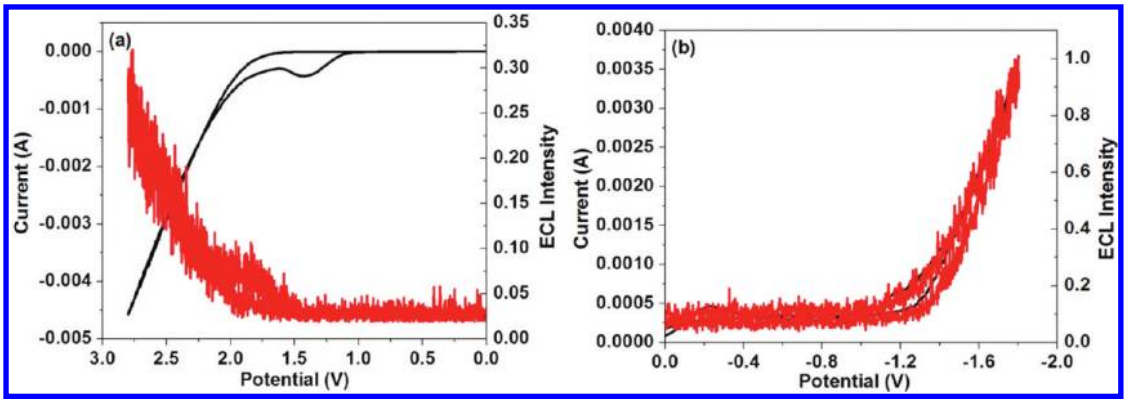

Figure 8. CVs of **Azide-BTA** NPs in aqueous 0.1 M $NaClO_4$ with (a) 0.1 M oxalate and (b) 0.1 M peroxydisulfate. WE: Pt disk. CE: Pt coil. RE: Ag/AgCl. Scan rate was 20 mV/s.

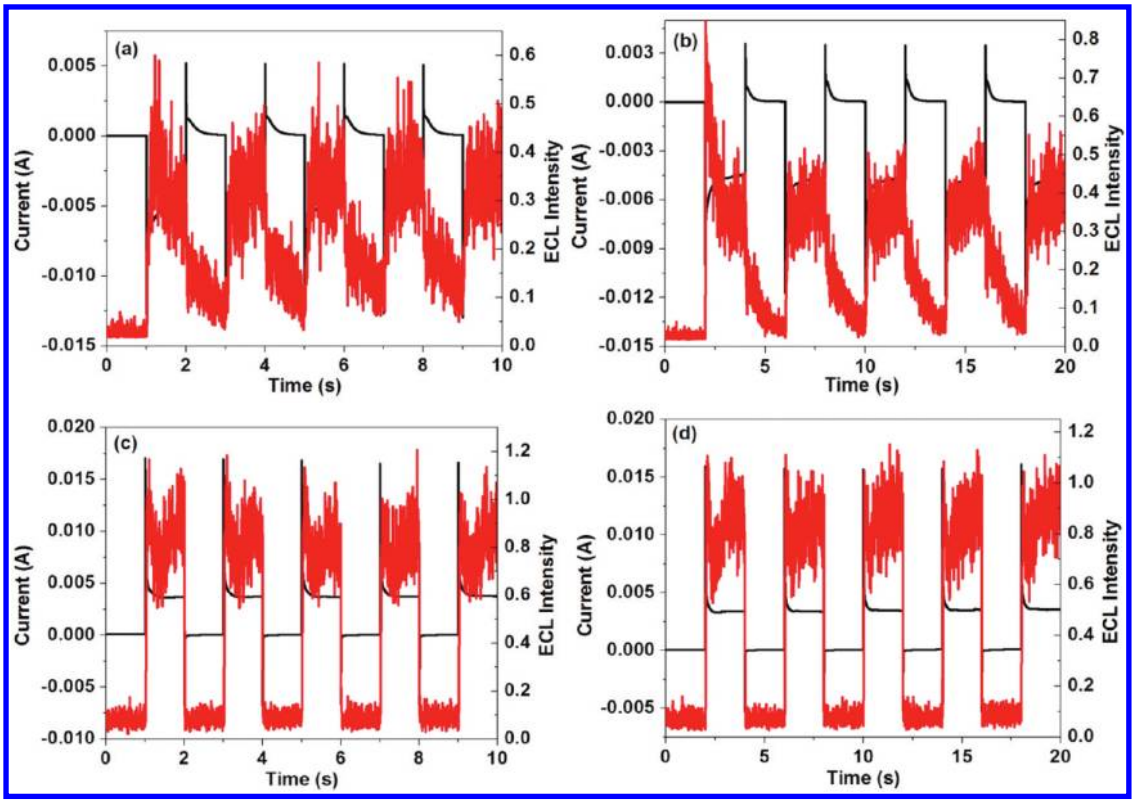

Figure 9. Transient ECL experiment, electrochemical current (black line), and ECL intensity (red line) for **Azide-BTA** NPs: (a) With 0.1 M oxalate; sampling time, 1 ms; pulsing pattern, 0−2.5 V; pulse width is 1 s. (b) With 0.1 M oxalate; sampling time, 1 ms; pulsing pattern, 0−2.5 V; pulse width is 2 s. (c) With 0.1 M peroxydisulfate; sampling time, 1 ms; pulsing pattern, 0 to −1.8 V; pulse width is 1 s. (d) With 0.1 M peroxydisulfate; sampling time, 1 ms; pulsing pattern, 0 to −1.8 V; pulse width is 2 s.

electrochemical features that could be clearly assigned to either the oxidation or reduction of the NPs themselves could not be distinguished in CVs of **Azide-BTA** NPs in water with 0.1 M $NaClO_4$; i.e., no distinctive peaks in the oxidation or reduction region could be seen. Moreover, the small diffusion coefficients of the relatively large NPs also contribute to small electrochemical signals. However, the ECL signal from the NPs in solution from PMT is more sensitive than the electrochemical signal for the **Azide-BTA** NPs. For NPs (16 ± 5 nm), ECL from the annihilation reaction was produced when the potential was first scanned negatively and then positively (Figure S9 in the Supporting Information). From scans like these, the limits for reduction and oxidation of the NPs can be roughly set at 1.5 and −1.8 V vs Ag/AgCl. Transient and weak ECL generated from annihilation was observed when the electrode potential was stepped from −2.2 to +2.3 V versus Ag/AgCl (Figure S10 in the Supporting Information). The ECL emission was stable with time, but the light intensity was not strong enough to obtain a spectrum with a CCD. Even though the size of NPs was small, with a low concentration and small diffusion coefficient, weak ECL could be observed.

We can also obtain information about the redox behavior and stronger ECL emission with a coreactant, either a reducing or

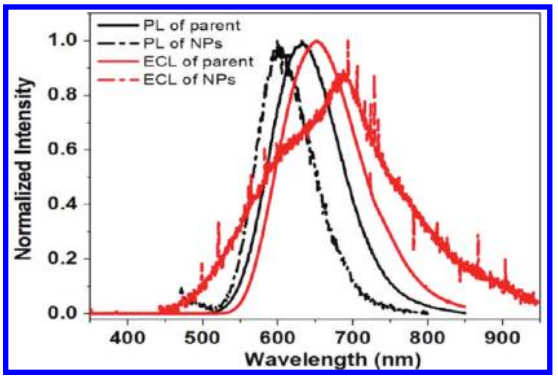

Figure 10. Fluorescence (black line) and ECL (red line) spectra of **Azide-BTA** and NPs. Solid line: **Azide-BTA** parent solution in 1:1 Bz: MeCN. Dotted line: **Azide-BTA** NPs dispersed in water. Slit width: 0.75 mm. Integration time: 5 min for ECL of parent solution, 10 min for ECL of NPs.

oxidizing one. Unlike Spiro-BTA,[10] tri-*n*-propylamine (TPrA) did not produce emission with **Azide-BTA** oxidation, probably because the intermediate radical is not a sufficiently strong reductant. However, the oxidation of **Azide-BTA** NPs with oxalate as a coreactant produced ECL emission by either a potential sweep or step. As shown in Figure 8(a), significant ECL emission was produced when the potential was scanned from 0 to +2.75 V to oxidize both the NPs and oxalate ion; the latter generates a strong reductant ($CO_2^{\bullet-}$). Transient ECL generated from the reaction of the oxidized NPs and the energetic reductive intermediate from oxalate oxidation was obtained by stepping the electrode potential with different pulse widths from 0.0 to +2.7 V versus Ag/AgCl (Figure 9(a) and (b)). No ECL was obtained when the electrode potential was stepped back to 0.0 V, as expected. The ECL signal was stable with time but was not strong enough to record an ECL spectrum. The low concentration and small diffusion coefficient of NPs and possible reactions between reducing agent and water or oxygen might cause only a very low intensity ECL signal.[30]

As shown in Figure 8(b), a much stronger ECL signal was observed when the potential was scanned from 0 to −1.8 V in 0.1 M $NaClO_4$ containing 0.1 M $K_2S_2O_8$ (a coreactant that forms a strong oxidizing agent, $SO_4^{\bullet-}$) ($E_{red} \geq 3.15$ V vs SCE).[31] Moreover, pulsing between 0 and −1.8 V produced strong ECL emission. Under these conditions, we could obtain an ECL spectrum (Figure 9(c) and (d)). The ECL spectrum (Figure 10, red dotted line) of the NPs showed a red emission peak at ∼670 nm, which is close to the ECL peak of **Azide-BTA** molecules (Figure 10, red solid line). The strong and broad ECL spectrum (with ∼200 nm half width) from NPs seems to consist of multiple peaks, perhaps from different sizes or different structures of the NPs. This is the first ECL spectrum obtained from organic NPs dispersed in water and suggests potential applications for organic NPs in aqueous media as ECL tags for analysis.

CONCLUSIONS

A new, red, highly fluorescent dye (**Azide-BTA**), a D−A−π−A−D molecule consisting of two triphenylamine groups as electron donors (D) and two 2,1,3-benzothiadiazole groups as electron acceptors (A) bridged by a fluorene moiety (π), has been synthesized and characterized. In addition, this molecule has azide groups attached to the fluorene moiety, which may be useful for future functionalization with a variety of species by click chemistry. **Azide-BTA** showed reversible oxidation and reduction waves in its CV and formed a stable dianion and dication. It shows a high PL quantum yield and produces strong and stable red ECL emission. In addition to studies of the dissolved **Azide-BTA**, we have successfully prepared, by a simple reprecipitation method, well-dispersed and spherical **Azide-BTA** NPs of diameter ∼16 ± 6 nm in water. ECL of **Azide-BTA** NPs by ion annihilation was produced with moderate intensity. The ECL from NPs with peroxydisulfate as the coreactant was bright and stable enough to record the ECL spectrum in water. Thus, organic NPs are potential labels for sensitive analytical methods in aqueous media.

ASSOCIATED CONTENT

Supporting Information. NMR spectra of products, scan rate studies, TEM images, absorption and emission spectra, and ECL data. This material is available free of charge via the Internet at http://pubs.acs.org.

AUTHOR INFORMATION

Corresponding Author

*E-mail: ajbard@mail.utexas.edu; kenwong@ntu.edu.tw.

ACKNOWLEDGMENT

We acknowledge support of this research from Roche Diagnostics, Inc., the National Science Foundation (CHE 0808927), and the Robert A. Welch Foundation (F-0021).

REFERENCES

(1) (a) Kubo, R. *J. Phys. Soc. Jpn.* **1962**, *17*, 975. (b) Brus, L. E. *J. Chem. Phys.* **1984**, *80*, 4403. (c) Hanamura, E. *Phys. Rev. B* **1988**, *37*, 1273. (d) Medintz, I. L.; Uyeda, H. T.; Goldman, E. R.; Mattoussi, H. *Nat. Mater.* **2005**, *4*, 435.

(2) (a) Peng, A.-D.; Xiao, D.-B.; Ma, Y.; Yang, W.-S.; Yao, J.-N. *Adv. Mater.* **2005**, *17*, 2070. (b) Patra, A.; Hebalkar, N.; Streedhar, B.; Sarkar, M.; Samanta, A.; Radhakrishnan, T. P. *Small* **2006**, *5*, 650. (c) Kaeser, A.; Schenning, A. P. H. J. *Adv. Mater.* **2010**, *22*, 2985.

(3) (a) Matsir, A. H.; Mizuno, K.; Nishi, O.; Matsushima, Y.; Shimizu, M.; Goto, T.; Takeshima, M. *Chem. Phys.* **1995**, *194*, 167. (b) Ye, J.; Chen, H.-Z.; Wang, M. *J. Mater. Sci.* **2003**, *38*, 4021.

(4) (a) Tamaki, Y.; Asahi, T.; Masuhara, H. *J. Phys. Chem. A* **2002**, *106*, 2135. (b) Tamaki, Y.; Asahi, T.; Masuhara, H. *Jpn. J. Appl. Phys.* **2003**, *42*, 2725. (c) Asahi, T.; Sugiyama, T.; Masuhara, H. *Acc. Chem. Res.* **2008**, *41*, 1790.

(5) Ibanez, A.; Maximov, S.; Guiu, A.; Chaillout, C.; Baldeck, P. L. *Adv. Mater.* **1998**, *10*, 1540.

(6) (a) Kasai, H.; Nalwa, H. S.; Oikawa, H.; Okada, S.; Matsuda, H.; Minami, N.; Kakuta, A.; Ono, K.; Mukoh, A.; Nakanishi, H. *Jpn. J. Appl. Phys. Part 2* **1992**, *31*, L1132. (b) Kasai, H.; Oikawa, H.; Okada, S.; Nakanishi, H. *Bull. Chem. Soc. Jpn.* **1998**, *71*, 2597. (c) Wu, C.; Peng, H.; Jiang, Y.; McNeill, J. *J. Phys. Chem. B* **2006**, *110*, 14148. (d) Kaneko, K.; Shimada, S.; Onodera, T.; Kimura, T.; Matsuda, H.; Okada, S.; Kasa, H.; Oikawa, H.; Kakudate, Y.; Nakanishi, H. *Jpn. J. Appl. Phys.* **2007**, *46*, 6893. (e) Mori, J.; Miyashita, Y.; Oliveira, D.; Kasai, H.; Oikawa, H.; Nakanishi, H. *J. Cryst. Growth* **2009**, *311*, 553.

(7) (a) Knight, A. W.; Greenway, G. M. *Analyst* **1994**, *119*, 879. (b) Richter, M. M. *Chem. Rev.* **2004**, *104*, 3003. (c) Miao, W. *Chem. Rev.* **2008**, *108*, 2506.

(8) (a) Ding, Z.; Quinn, B. M.; Haram, S. K.; Pell, L. E.; Korgel, B. A.; Bard, A. J. *Science* **2002**, *296*, 1293. (b) Bard, A. J.; Ding, Z.; Myung, N.

Struct. Bonding (Berlin, Ger.) **2005**, *118*, 1. (c) Myung, N.; Lu, X.; Johnston, K. P.; Bard, A. J. *Nano Lett.* **2004**, *4*, 183. (d) Myung, N.; Lu, X.; Ding, Z.; Bard, A. J. *Nano Lett.* **2004**, *2*, 1315. (e) Ren, T.; Xu, J.-Z.; Tu, Y.-F.; Xu, S.; Zhu, J.-J. *Electrochem. Commun.* **2005**, *7*, 5. (f) Chen, M.; Pan, L.; Huang, Z.; Cao, J.; Zheng, Y.; Zhang, H. *Mater. Chem. Phys.* **2007**, *101*, 317. (g) Shen, L.; Cui, X.; Qi, H.; Zhang, C. *J. Phys. Chem. C* **2007**, *111*, 8172.

(9) Omar, K. M.; Bard, A. J. *J. Phys. Chem. C* **2009**, *113*, 11575.

(10) Omer, K. M.; Ku, S. Y.; Cheng, J. Z.; Chou, S. H.; Wong, K. T.; Bard, A. J. *J. Am. Chem. Soc.* **2011**, *113*, 5492.

(11) Liu, B.; Dishari, S. K. *Chem.—Eur. J.* **2008**, *14*, 7366.

(12) Pu, K.-Y.; Fang, Z.; Liu, B. *Adv. Funct. Mater.* **2008**, *18*, 1321.

(13) Sahami, S.; Weaver, M. *J. Electroanal. Chem.* **1981**, *122*, 155.

(14) Omar, K. M.; Ku, S.-Y.; Chen, Y.-C.; Wong, K.-T.; Bard, A. J. *J. Am. Chem. Soc.* **2010**, *132*, 10944.

(15) Yasuda, T.; Imase, T.; Yamamaoto, T. *Macromolecules* **2005**, *38*, 7378.

(16) Zhan, X.; Liu, Y.; Zhu, D.; Huang, W.; Gong, Q. *J. Phys. Chem. B* **2002**, *106*, 1884.

(17) Chien, Y.-Y.; Wong, K.-T.; Chou, P.-T.; Cheng, Y.-M. *Chem. Commun.* **2002**, *23*, 2874.

(18) Fonseca, S. M.; Pina, J.; Arnaut, L. G.; Melo, S.; Burrows, H. D.; Chattopadhyay, N.; Alcacer, L.; Morgado, C. J.; Monkman, A. P.; Asawapirom, U.; Scherf, U.; Edge, R.; Navaratnam, S. *J. Phys. Chem. B* **2006**, *110*, 8278.

(19) Sartin, M. M.; Camerel, F.; Ziessel, R.; Bard, A. J. *J. Phys. Chem. C* **2008**, *112*, 10833.

(20) (a) Chandross, E.; Sonntag, F. *J. Am. Chem. Soc.* **1966**, *88*, 1089. (b) Santa Cruz, T. D.; Akins, D. L.; Brike, R. L. *J. Am. Chem. Soc.* **1976**, *98*, 1677.

(21) (a) Faulkner, L. R.; Bard, A. J. *Electroanalytical Chemistry*; Bard, A. J., Ed.; Dekker: New York, 1977; Vol. 10, pp 1−95. (b) Faulkner, L. R.; Glass, R. S. In *Chemical and Biological Generation of Excited States*; Waldemar, A., Giuseppe, C., Eds.; Academic Press: New York, 1982; Chapter 6. (c) Bard, A. J.; Debad, J. D.; Leland, J. K.; Sigal, G. B.; Wilbur, J. L.; Wohlstadter, J. N. In *Encyclopedia of Analytical Chemistry: Applications, Theory and Instrumentation*; Meyers, R. A., Ed.; John Wiley & Sons: New York, 2000; Vol. 11, p 9842. (d) Bard, A. J., Ed. *Electrogenerated Chemiluminescence*; Marcel Dekker: New York, 2004.

(22) Marcus, R. A. *J. Phys. Chem.* **1989**, *93*, 3078.

(23) (a) Qian, L. J.; Tong, B.; Shen, J. B.; Shi, J. B.; Zhi, J. G.; Dong, Y. Q.; Yang, F.; Dong, Y. P.; Lam, J. W. Y.; Liu, Y.; Tang, B. *J. Phys. Chem. B* **2009**, *113*, 9098. (b) Tang, B. Z.; Geng, Y. H.; Lam, J. W. Y.; Li, B. S.; Jing, X. B.; Wang, X. H.; Wang, F. S.; Pakhomov, A. B.; Zhang, X. X. *Chem. Mater.* **1999**, *11*, 1581. (c) Lu, L. D.; Helgeson, R.; Jones, R. M.; McBranch, D.; Whitten, D. *J. Am. Chem. Soc.* **2002**, *124*, 483. (d) Feng, X.; Tong, B.; Shen, J.; Shi, J.; Han, T.; Chen, L.; Zhi, J.; Lu, P.; Ma, Y.; Dong, Y. *J. Phys. Chem. B* **2010**, *114*, 16736.

(24) Kasai, H.; Kamatani, H.; Okada, S.; Oikawa, H.; Matsuda, H.; Nakanishi, H. *Jpn. J. Appl. Phys.* **1996**, *34*, L221.

(25) Kasai, H.; Kamatani, H.; Yoshikawa, Y.; Okada, S.; Oikawa, H.; Watanabe, A.; Ito, O.; Nakanishi, H. *Chem. Lett.* **1997**, 1181.

(26) Kasai, H.; Yoshikawa, Y.; Seko, T.; Okada, S.; Oikawa, H.; Matsuda, H.; Watanabe, A.; Ito, O.; Toyotama, H.; Nakanishi, H. *Mol. Cryst. Liq. Cryst.* **1997**, *294*, 173.

(27) Komai, Y.; Kasai, H.; Hirakoso, H.; Hakuta, Y.; Okada, S.; Oikawa, H.; Adschiri, T.; Inomata, H.; Arai, K.; Nakanishi, H. *Mol. Cryst. Liq. Cryst.* **1998**, *322*, 167.

(28) Fu, H.-B.; Yao, J.-N. *J. Am. Chem. Soc.* **2001**, *123*, 1434.

(29) (a) An, B.; Kwon, S.; Jung, S.; Park, S. Y. *J. Am. Chem. Soc.* **2002**, *124*, 14410. (b) Feng, X.; Tong, B.; Shi, J.; Han, T.; Chen, L.; Xhi, J.; Lu, P.; Ma, Y.; Dong, Y. *J. Phys. Chem. B* **2010**, *114*, 16731.

(30) Omer, K. M.; Bard, A. J. *J. Phys. Chem. C* **2009**, *113*, 11575.

(31) Memming, R. *J. Electrochem. Soc.* **1969**, *116*, 785.